



# CHORUS

This is the accepted manuscript made available via CHORUS. The article has been published as:

## Liquid Structure of Shock-Compressed Hydrocarbons at Megabar Pressures

N. J. Hartley, J. Vorberger, T. Döppner, T. Cowan, R. W. Falcone, L. B. Fletcher, S. Frydrych, E. Galtier, E. J. Gamboa, D. O. Gericke, S. H. Glenzer, E. Granados, M. J. MacDonald, A. J. MacKinnon, E. E. McBride, I. Nam, P. Neumayer, A. Pak, K. Rohatsch, A. M. Saunders, A. K. Schuster, P. Sun, T. van Driel, and D. Kraus

Phys. Rev. Lett. **121**, 245501 — Published 14 December 2018

DOI: [10.1103/PhysRevLett.121.245501](https://doi.org/10.1103/PhysRevLett.121.245501)

# Liquid Structure of Shock-Compressed Hydrocarbons at Megabar Pressures

N. J. Hartley,<sup>1,2,\*</sup> J. Vorberger,<sup>1</sup> T. Döppner,<sup>3</sup> T. Cowan,<sup>1,4</sup> R. W. Falcone,<sup>5</sup> L. B. Fletcher,<sup>6</sup> S. Frydrych,<sup>7,3</sup> E. Galtier,<sup>6</sup> E. J. Gamboa,<sup>6</sup> D. O. Gericke,<sup>8</sup> S. H. Glenzer,<sup>6</sup> E. Granados,<sup>6</sup> M. J. MacDonald,<sup>6,9</sup> A. J. MacKinnon,<sup>6</sup> E. E. McBride,<sup>6,10</sup> I. Nam,<sup>6</sup> P. Neumayer,<sup>11</sup> A. Pak,<sup>3</sup> K. Rohatsch,<sup>1</sup> A. M. Saunders,<sup>5</sup> A. K. Schuster,<sup>1</sup> P. Sun,<sup>6</sup> T. van Driel,<sup>6</sup> and D. Kraus<sup>1,4</sup>

<sup>1</sup>*Helmholtz-Zentrum Dresden-Rossendorf, Bautzner Landstraße 400, Dresden 01328, Germany*

<sup>2</sup>*Open and Transdisciplinary Research Institute, Osaka University, Suita, Osaka 565-0871, Japan*

<sup>3</sup>*Lawrence Livermore National Laboratory, Livermore CA 94550, USA*

<sup>4</sup>*Technische Universität Dresden, Dresden 01062, Germany*

<sup>5</sup>*Department of Physics, University of California, Berkeley CA 94720, USA*

<sup>6</sup>*SLAC National Accelerator Laboratory, Menlo Park CA 94309, USA*

<sup>7</sup>*Technische Universität Darmstadt, Schlossgartenstraße 9, 64289 Darmstadt, Germany*

<sup>8</sup>*Centre for Fusion, Space and Astrophysics, Department of Physics, University of Warwick, Coventry CV4 7AL, United Kingdom*

<sup>9</sup>*University of Michigan, Ann Arbor, MI 48109, USA*

<sup>10</sup>*European XFEL GmbH, Holzkoppel 4, 22869 Schenefeld, Germany*

<sup>11</sup>*GSI Helmholtzzentrum für Schwerionenforschung GmbH, Planckstraße 1, 64291 Darmstadt, Germany*

(Dated: November 7, 2018)

We present results for the ionic structure in hydrocarbons (polystyrene, polyethylene) that were shock compressed to pressures of up to 190 GPa, inducing rapid melting of the samples. The structure of the resulting liquid is then probed using *in situ* diffraction by an X-ray free electron laser beam, demonstrating the capability to obtain reliable diffraction data in a single shot, even for low-Z samples without long range order. The data agrees well with *ab initio* simulations, validating the ability of such approaches to model mixed samples in states where complex interparticle bonds remain, and showing that simpler models are not necessarily valid. While the results clearly exclude the possibility of complete carbon-hydrogen demixing at the conditions probed, they also, in contrast to previous predictions, indicate that diffraction is not always a sufficient diagnostic for this phenomenon.

Compounds and mixtures containing low-Z elements at high pressures and temperatures are relevant to a variety of scientific fields, including the modelling giant planets [2–4], geophysics [5, 6] and inertial confinement fusion research [7, 8]. Such matter often includes hydrocarbons which, being formed from some of the most common elements in the universe, are a major constituent of ‘icy giant’ planets [9]. In the form of plastics, hydrocarbons are also used as ablator materials in high energy density (HED) research [10], and to drive the compression in inertial confinement fusion (ICF) implosions [11].

Describing initially covalently bound compounds at high pressures and temperatures is generally complex, because the thermal energy is comparable to the binding energy, such that the lifetimes of chemical bonds are reduced – although the bonds do not break completely – and long range order is lost. It may also be energetically favourable for the mixture of atom types to demix into separate phases with different atomic ratios [12], as has been shown with hydrogen and helium in giant planet interiors [13, 14], or the formation of diamonds within icy giant planets [15, 16]. Such demixing strongly influences the mass and energy transport in planetary mantles, with consequences for the evolution and cooling rate [17]. If similar processes occur in ICF ablaters, the resulting higher density liquid, or solid material, could be

the source of hydrodynamic instabilities and ablator-fuel mixing at the interface [18].

While high pressure matter inside planets is gravitationally contained [19], recreating such conditions in the laboratory is challenging; although static compression techniques are able to cover an increasingly large region of pressure-temperature space [20, 21], the highest pressures can only be reached through dynamic compression. These can include magnetically driven flyer plates [22] or, as in the work presented here, laser-driven shock compression [23]. While this does create high pressure and temperature states, they occur only briefly. The sample must therefore be studied within the confinement time, which is on the order of ns for laser-driven shock compression.

One of the most successful approaches to studying such highly transient states uses fs-scale X-ray pulses from X-ray Free Electron Lasers (XFELs) to probe the structure of the ions within a sample by diffraction [24]. Due to the short lifetime of the conditions reached in dynamic experiments, it is essential that this data can be reliably obtained from a single shot. This becomes even more important for laser-driven experiments, where significant shot-to-shot variation in the laser energy or pulse shape may occur. Obtaining single-shot data is well-established for mid- to high-Z materials, which give strong diffraction

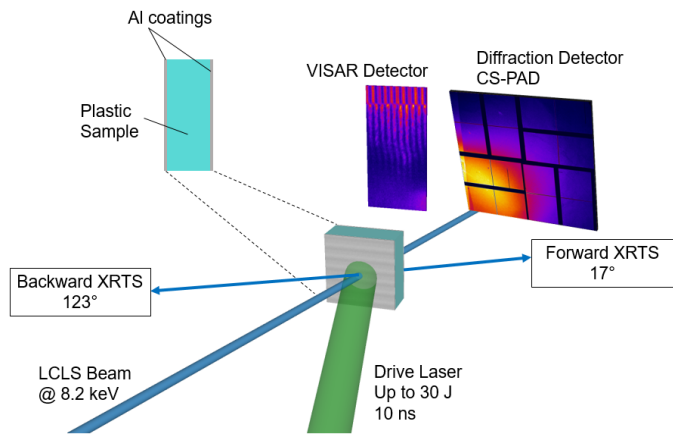


FIG. 1: Schematic of the experimental setup at the MEC endstation of LCLS. The high energy laser beam irradiates a plastic sample - either CH ( $83 \mu\text{m}$  polystyrene) or  $\text{CH}_2$  ( $77 \mu\text{m}$  polyethylene) - driving a shock into the target. The conditions reached were monitored by a VISAR setup, and the compressed sample was probed by a single X-ray pulse at 8.2 keV. The scattered X-ray signal was observed by the large area CS-PAD detector.

signals [25–27], and crystalline structures, which contain clear Bragg peaks [28]. Data from low-Z materials in the liquid state had until recently only been possible by accumulating data over many shots [29], but have now been seen in single-shot data [15, 16] allowing direct comparison with simulation.

In this Letter, we show single-shot diffraction data from shock-compressed hydrocarbons at the Linac Coherent Light Source (LCLS). The results are compared to predictions from density functional theory molecular dynamics (DFT-MD) simulations, demonstrating excellent agreement at two different pressure conditions within the HED regime.

Our experiment was performed at the Matter in Extreme Conditions endstation of LCLS at Stanford National Accelerator Laboratory. Figure 1 shows a schematic of the experiment setup used. Samples of CH ( $83 \mu\text{m}$  polystyrene) and  $\text{CH}_2$  ( $76 \mu\text{m}$  polyethylene) were irradiated by either one or both of the long pulse (10 ns) lasers, with intensities of  $\sim 2 \times 10^{12}$  to  $1 \times 10^{13} \text{ W/cm}^2$  showing shot-to-shot variation of  $\sim 10\%$ . The samples are coated on both sides with aluminum; the rear, in order to provide a reflective surface for diagnosing with the Velocity Interferometer System for Any Reflector (VISAR), and on the front to prevent prepulses from disturbing this reflective layer.

The temperature and pressure conditions expected in the experiment were simulated hydrodynamically using the code package MULTI with the SESAME equation of

state tables 7592, for CH, and 7171, for  $\text{CH}_2$ . The measured laser profiles for shots with one or both of the lasers gave pressures on the order of  $\sim 60$  and  $\sim 190 \text{ GPa}$ , with temperatures of  $\sim 2000$  and  $\sim 10,000 \text{ K}$ , respectively, results which are in good agreement with experimental equation of state measurements [30–32]. The pressure estimates on each shot were also confirmed using a combination of the X-ray diffraction data and the VISAR fringe shift and breakout timing results. Further details are given in the Supplementary Material [1] (citing [33, 34]), and in our previous publication [15].

The sample was probed by the XFEL beam close to the breakout time of the shock, such that the conditions were as uniform as possible and maximising the volume of shocked material. In all cases, the shock breakout time was shorter than the laser pulse length, such that the shock was supported throughout the time it traversed the sample. The diffracted signal was observed on a Cornell-SLAC Pixel Array Detector (CS-PAD), covering an angular range of  $20^\circ$ – $90^\circ$ . This detector is not able to distinguish elastic and inelastic scattering at a given angle, so to account for the relative contributions, the MCSS (Multicomponent Scattering Simulation) code [35, 36, 53] was used to calculate the inelastic signal as a function of the scattering angle, which was added to the calculated elastic signal (see Supplementary Material [1], including reference [37–39]). To validity of this approach was checked by comparing the predicted spectra were compared to results from X-ray Thomson Scattering (XRTS) spectrometers, deployed at fixed angles ( $17^\circ$  and  $123^\circ$ ), where we found good agreement for the total signal.

The elastic scattering is due to coherent scatter from the ions within the sample, allowing for a direct comparison of diffraction measurements and theoretical or simulated results for the microscopic ion structure. The X-ray intensity elastically scattered from the sample is determined by the Rayleigh weight [12]

$$W_R(k) = \sum_{a,b} \sqrt{x_a x_b} f_a(k) f_b(k) S_{ab}(k). \quad (1)$$

Here, the form factor  $f_i(k)$  describes the distribution of bound electrons around the ions, the ion structure in our multi-component system is given by the partial ion-ion structure factors  $S_{ab}(k)$  and  $x_a$  is the number ratio of the species  $x_a = N_a / \sum_i N_i$ . The expression above ignores the effect of free electrons screening the ions as we have negligible ionisation at the conditions considered [24]. The wavenumber  $k$  is related to the experimental parameters via  $k = (4\pi/\lambda) \sin(\theta/2)$ , where  $\lambda$  is the wavelength of the probing X-rays and  $\theta$  the scattering angle.

The values for the theoretical predictions of the Rayleigh weight  $W_R$  were obtained from first principle simulations (DFT-MD). For this work, we employ the VASP package [40–43] (see Ref. [1] for details, including references [54–59]). These runs yield the positions of the

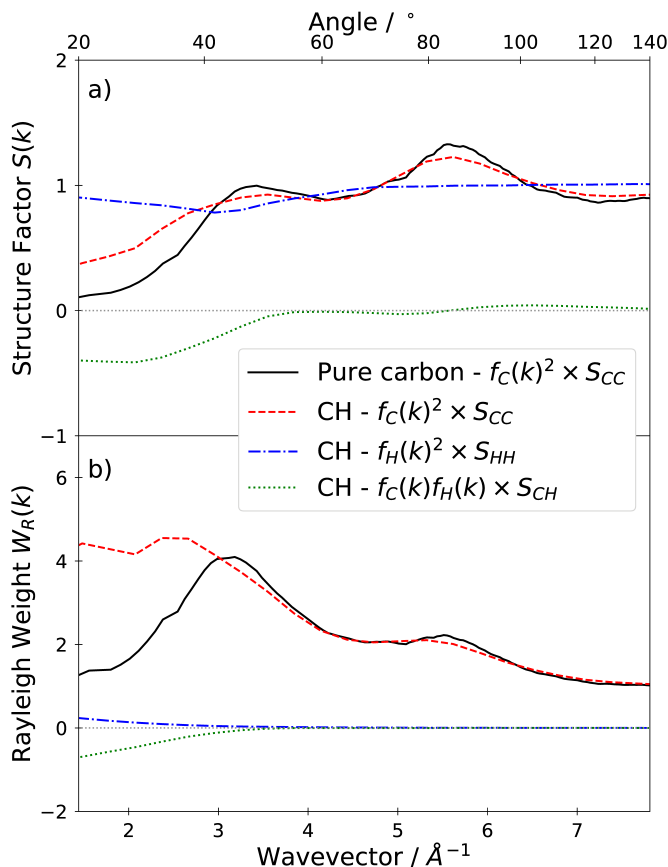


FIG. 2: Simulated values for the a) structure factor and b) partial and total Rayleigh weights from CH and pure carbon simulations, respectively. Both are simulated at 190 GPa and 10,000 K, with the carbon-carbon component exhibiting the characteristic two-peak structure, although the screening effect of the hydrogen in the mixed case leads to less strong correlations. The carbon-carbon correlations dominate the Rayleigh weight due to the form factors of the atoms  $f(k)$ , which are proportional to the electron numbers.

atoms at each timestep, which can then be Fourier transformed to give the static structure factors  $S_{ab}(k)$ , describing the spatial correlation between the species ( $a, b$ ) in equilibrium, including both the self-correlation  $S_{CC}$ ,  $S_{HH}$  and inter-species correlation  $S_{CH}$ .

Figure 2 shows the structure factors and Rayleigh weights for a pure carbon sample (solid line), and for the different components of a CH sample (dashed lines). The two-peak structure is characteristic of liquid carbon [44], and is due to residual bonding that persists after melting. In the case of CH, a similar shape can be seen in the carbon-carbon structure factor, which dominates the overall signal of the Rayleigh weight due to the much larger form factor of carbon, relative to hydrogen. Such a structure does not appear when simpler models, such as

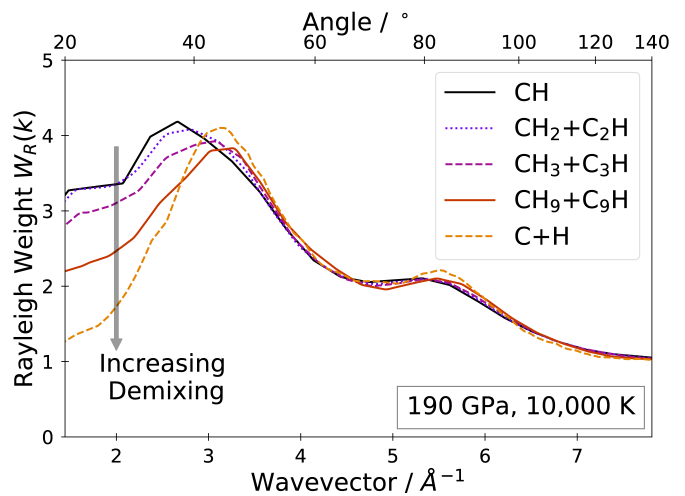


FIG. 3: Simulated values for the Rayleigh weight from a CH sample with increasing degrees of demixing, at 190 GPa and 10,000 K. For moderate degrees of demixing, the change in the total signal is too small to be confidently distinguished from the completely mixed case.

Yukawa potentials, are used [44, 45], despite their success in describing other materials at HED conditions [26, 46].

When comparing the simulation results to the experimental data, we initially considered only a fully mixed fluid sample or a fully demixed sample, with regions of pure liquid carbon and others of pure liquid hydrogen. Demixing into solid carbon, as was seen at conditions away from the shock Hugoniot [15, 16], was not considered, as no Bragg peaks from a diamond structure were observed with the single shocks used in our experiment. For this fully demixed case, the expected diffraction signal can be approximated by adding simulated contributions of pure carbon and pure hydrogen, weighted by the appropriate atomic fractions. In practice, this result is indistinguishable from the pure carbon sample, as the lower Z hydrogen atoms contribute negligible signal.

Similar simulations were performed for samples with different carbon-hydrogen ratios. As was done for the fully demixed case described above, outputs from two simulations with different C/H ratios were added, with appropriate weightings to give the correct overall composition [1]. These results are shown in Figure 3, for fully mixed CH (from a single simulation) and increasingly asymmetrically demixed regions (summing two simulations). We see that, as the material demixes, the first peak sharpens and the signal at low  $k$  decreases, approaching that of a fully demixed sample i.e. a pure carbon liquid. However, this change only becomes significant when the ratio in the carbon region is above 3:1, and so moderate levels of demixing cannot be distinguished by diffraction in this material. A similar ambiguity is

found for the case of  $\text{CH}_2$ .

We should stress that in none of the simulations performed was spontaneous demixing observed, and that therefore all of the ‘demixed’ theoretical results are obtained as combinations of mixed results with different atomic ratios. The absence of spontaneous demixing may be caused by the relatively small number of particles considered (several hundred) and the limited runtime (several tens of picoseconds). Both limitations strongly reduce the probability of the system to spontaneously overcome the initial energy barrier for demixing, due to the considerable covalent bond strengths.

The experimental results are shown as solid lines in Figure 4, with the shaded region showing the range of shots at the same nominal laser drive conditions. To directly compare the simulated and experimental data, the DFT-MD data (Rayleigh peak) also includes the modeled effect of the angle-dependent inelastic scattering, as discussed above. The experimental data is scaled to remove the effect of absorption within the target and the detector shielding. The effect of the polarization of the probing XFEL beam was accounted for in the Dioptas software [47] used to analyse the CS-PAD data.

Looking first at the pre-shock (cold) data (dotted lines in Figure 4), it is apparent that the CH has no Bragg peaks, and its signal is dominated by a steep rise in signal at low angles, whereas the  $\text{CH}_2$  has a complex crystal structure, primarily orthorhombic  $Pnam$  [48]. In both cases, Bragg diffraction lines from the thin (100 nm) Al layers on either side of the target are also seen, marked by \*. These peaks disappear completely in shots probing after the shock has broken out the rear side of the sample.

After compression, the structures in both materials are more similar, with all data except Figure 4d) showing a liquid structure with two broad peaks in the angular range probed. The exception to this behaviour is the case of weakly shocked  $\text{CH}_2$  where at least three new peaks (marked by †) are present in the lineout. These new peaks appear to be due to a monoclinic  $A2/m$  crystal structure, which was previously found to be the most stable structure above 14 GPa [48]. The lattice parameters were taken from this work and are scaled hydrostatically to fit the observed peaks.

The  $\text{CH}_2$  data at both pressures also contains obvious signal from the initial crystal structure, with the Bragg peaks at  $21^\circ$  and  $23^\circ$  still particularly visible. This signal is due to a ‘halo’ of X-rays around the focal spot, comprising  $\sim 5\%$  of the total fluence, which gives diffraction signal from cold material outside the shocked region even at long delays. This cold signal also appeared in the CH shots, but has been subtracted to better demonstrate the fitting with the theoretical lineouts. It was not practical to subtract it from the  $\text{CH}_2$  shots due to the complexity and irreproducibility of the crystal structure.

The two-peak liquid structures predicted by the DFT-MD simulations are very similar to those present in the data for all the target/pressure combinations where liquid structure dominates. This similarity indicates that carbon-carbon bonding continues to strongly influence the behaviour [49, 50]. The shapes, positions and heights of the liquid peaks in the simulations agree very closely with the measured lineouts, although this is true for both fully and partially mixed simulations. The fully demixed case diverges significantly from the data at low  $k$ , and therefore such extreme demixing behaviour can be ruled out. In the weakly shocked  $\text{CH}_2$ , the data agrees at higher angles, where smaller scale effects dominate, but at lower angles there is a clear redistribution of signal from the broad liquid peak into specific lattice peaks, which were not present in the DFT-MD simulations.

Although previous work had suggested that diffraction would be an appropriate technique to observe demixing in liquid-like warm dense matter [12], our comparison demonstrates that this is not necessarily the case. For the materials and conditions probed, the total structure factor changes very little with moderate demixing, i.e. regions with an atomic imbalance of up to around 3:1. For strongly shocked CH, the simulated Rayleigh weight defined in Equation (1) is plotted for different degrees of demixing in Figure 3. At ratios in the carbon-enriched region of up to 3:1, the maximum change in signal is on the order of 10%. Our data can rule out regions with carbon ratios above  $\text{C}_9\text{H}$  at the conditions reached. However, weaker demixing effects are still sufficient to give density variations that could, for instance, seed observed instabilities and fuel-ablator mixing in ICF capsule implosions [7, 11, 18]. While diffraction cannot distinguish the small differences in structure between these regions, diagnostics sensitive to density gradients, such as SAXS [52], may be useful for better constraining this in the future.

To conclude, we have used X-ray diffraction to observe the microscopic ion structure of fluid hydrocarbons. Our results demonstrate that single-shot data can be obtained even in low-Z materials without strong structural order. At pressure-temperature conditions reached by a single shock in CH targets, the liquid structure agrees very well with predictions from DFT-MD simulations. The two-peak shape of the diffraction signal demonstrates the importance of complex covalent bonding that persists in carbon at HED conditions. In  $\text{CH}_2$ , crystalline structures are observed at pressures around 60 GPa on the timescales probed in this experiment, but do not remain at 190 GPa. Overall, our results are good validation for the predictive power of DFT-MD simulations for the complex liquid structure in HED mixtures. It also highlights the potential of finding novel structures in other low-Z elements and compounds at planetary interior conditions. While the lack of complete demixing suggests it

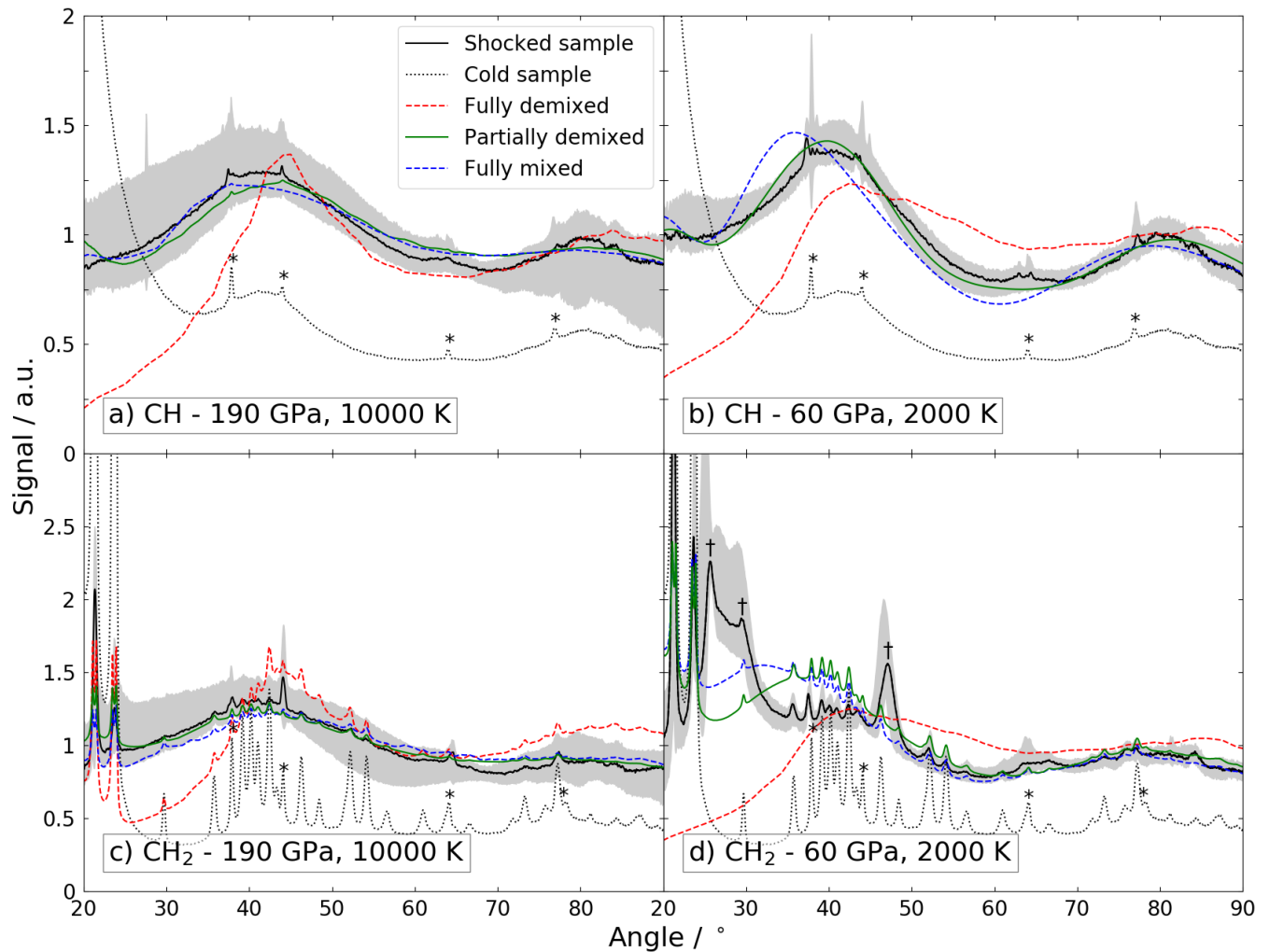


FIG. 4: Azimuthally integrated lineouts of the diffraction data from the CS-PAD, compared to DFT-MD simulations with mixed and demixed hydrocarbons. The black lines show single shots, and the shaded regions around them indicate the range of data at similar shock conditions; the conditions given in each Figure are those of the DFT-MD simulations, which fall within the uncertainty of the experimental conditions. The partially demixed result is the best-fitting case of the combinations shown in Figure 3 at the appropriate conditions. The dotted line indicates the initial structure of the sample, before laser irradiation, with peaks from aluminum marked by \*. In the case of the lower pressure  $\text{CH}_2$  data, locations of Bragg peaks attributed to the monoclinic  $A2/m$  structure are indicated by †.

may not have a strong impact on ICF implosions using plastic ablaters, we cannot rule out other chemical activity and partial demixing. Determining weak partial demixing will require additional diagnostics.

This work was performed at the Matter at Extreme Conditions (MEC) endstation of the Linac Coherent Light Source (LCLS), SLAC National Accelerator Laboratory, supported by the U.S. Department of Energy (DOE), Office of Science, Office of Basic Energy Sciences under Contract No. DE-AC02-76SF00515. The MEC instrument has additional support from the DOE, Office of Science, Office of Fusion Energy Sciences under con-

tract No. SF00515. N.J.H., K.R., A.K.S. and D.K. were supported by the Helmholtz Association under VH-NG-1141. N.J.H. was supported in part by JSPS KAKENHI Grant No. 16K17846. The work of T.D., A.P. and S.F. was performed under the auspices of the U.S. Department of Energy by Lawrence Livermore National Laboratory under Contract DE-AC52-07NA27344. We acknowledge support by DOE FES through FWP 1001182. T.D. was supported by Laboratory Directed Research and Development (LDRD) Grant No. 18-ERD-033. S.F. was supported by Bundesministerium für Bildung und Forschung (BMBF) with project no. 05P15RDFA1. The MCSS code is (C) British Crown Owned Copyright 2017/AWE

and is used with permission.

- 
- \* n.hartley@hzdr.de
- [1] Supplementary Material
  - [2] N. Nettelmann, *Astrophysics and Space Science* 336 (1) (2011) 47–51.
  - [3] F. Soubiran, B. Militzer, K. P. Driver, S. Zhang, *Physics of Plasmas* 24 (4) (2017) 041401.
  - [4] M. Millot, S. Hamel, J. R. Rygg, P. M. Celliers, G. W. Collins, F. Coppari, D. E. Fratanduono, R. Jeanloz, D. C. Swift, J. H. Eggert, *Nature Physics* 14 (2018) 297–302.
  - [5] H. K. Mao, Y. Wu, L. C. Chen, J. F. Shu, A. P. Jephcoat, *Journal of Geophysical Research* 95 (B13) (1990) 737–742.
  - [6] D. K. Spaulding, R. S. McWilliams, R. Jeanloz, J. H. Eggert, P. M. Celliers, D. G. Hicks, G. W. Collins, R. F. Smith, *Physical Review Letters* 108 (6) (2012) 065701.
  - [7] R. S. Craxton, K. S. Anderson, T. R. Boehly, V. N. Goncharov, D. R. Harding, J. P. Knauer, R. L. McCrory, P. W. McKenty, D. D. Meyerhofer, J. F. Myatt, A. J. Schmitt, J. D. Sethian, R. W. Short, S. Skupsky, W. Theobald, W. L. Kruer, K. Tanaka, R. Betti, T. J. B. Collins, J. A. Delettrez, S. X. Hu, J. A. Marozas, A. V. Maximov, D. T. Michel, P. B. Radha, S. P. Regan, T. C. Sangster, W. Seka, A. A. Solodov, J. M. Soures, C. Stoeckl, J. D. Zuegel, *Physics of Plasmas* 22 (11) (2015) 110501.
  - [8] A. L. Kritcher, T. Döppner, D. Swift, J. A. Hawreliak, G. Collins, J. Nilsen, B. L. Bachmann, E. Dewald, D. Strozzi, S. Felker, O. L. Landen, O. Jones, C. Thomas, J. Hammer, C. Keane, H. Lee, S. H. Glenzer, S. Rothman, D. A. Chapman, D. Kraus, P. Neumayer, R. W. Falcone, *High Energy Density Physics* 10 (2014) 27–34.
  - [9] W. B. Hubbard, W. J. Nellis, A. C. Mitchell, N. C. Holmes, P. C. McCandless, S. S. Limaye, *Science* 253 (5020) (1991) 648.
  - [10] I. Prencipe, J. Fuchs, S. Pascarelli, D. Schumacher, R. Stephens, N. B. Alexander, R. Briggs, M. Büscher, M. Cernaianu, A. Choukourov, M. De Marco, A. Erbe, J. Fassbender, G. Fiquet, P. Fitzsimmons, C. Georghiu, J. Hund, L. Huang, M. Harmand, N. J. Hartley, A. Irman, T. Kluge, Z. Konopkova, S. Kraft, D. Kraus, V. Leca, D. Margarone, J. Metzkes, K. Nagai, W. Nazarov, P. Lutoslawski, D. Papp, M. Passoni, A. Pelka, J. Perin, J. Schulz, M. Smid, C. Spindloe, S. Steinke, R. Torchio, C. Vass, T. Wiste, R. Zaffino, K. Zeil, T. Tschentscher, U. Schramm, T. Cowan, *High Power Laser Science and Engineering* 5 (e17) (2017).
  - [11] A. Kritcher, D. Clark, S. Haan, S. Yi, A. Kritcher, S. Haan, S. Yi, A. Zylstra, J. Ralph, C. Weber, *Tech. rep.* (2017).
  - [12] K. Wünsch, J. Vorberger, G. Gregori, D. O. Gericke, *EPL* 94 (2011) 25001.
  - [13] M. A. Morales, S. Hamel, K. J. Caspersen, E. Schwegler, *Physical Review B* 87 (17) (2013) 5–8.
  - [14] N. Nettelmann, B. Holst, A. Kietzmann, M. French, R. Redmer, D. Blaschke, *The Astrophysical Journal* 683 (2) (2008) 1217–1228.
  - [15] D. Kraus, J. Vorberger, A. Pak, N. J. Hartley, L. B. Fletcher, S. Frydrych, E. Galtier, E. J. Gamboa, D. O. Gericke, S. H. Glenzer, E. Granados, M. J. MacDonald, A. J. MacKinnon, E. E. McBride, I. Nam, P. Neumayer, M. Roth, A. M. Saunders, A. K. Schuster, P. Sun, T. van Driel, T. Döppner, R. W. Falcone, *Nature Astronomy* 1 (September) (2017).
  - [16] D. Kraus, N. J. Hartley, S. Frydrych, A. K. Schuster, K. Rohatsch, M. Rödel, T. E. Cowan, S. Brown, E. Cunningham, T. van Driel, L. B. Fletcher, E. Galtier, E. J. Gamboa, A. Laso Garcia, D. O. Gericke, E. Granados, P. A. Heimann, H. J. Lee, M. J. MacDonald, A. J. MacKinnon, E. E. McBride, I. Nam, P. Neumayer, A. Pak, A. Pelka, I. Prencipe, A. Ravasio, R. Redmer, A. M. Saunders, M. Schölmerich, M. Schörner, P. Sun, S. J. Turner, A. Zetzel, R. W. Falcone, S. H. Glenzer, T. Döppner, J. Vorberger, *Physics of Plasmas* 25 (5) (2018) 056313.
  - [17] M. Schöttler, R. Redmer, *Physical Review Letters* 120 (11) (2018) 115703.
  - [18] C. D. Orth, *Physics of Plasmas* 23 (2) (2016) 022706.
  - [19] N. Nettelmann, K. Wang, J. J. Fortney, S. Hamel, S. Yellamilli, M. Bethkenhagen, R. Redmer, *Icarus* 275 (2016) 107–116.
  - [20] L. Dubrovinsky, N. Dubrovinskaia, V. B. Prakapenka, A. M. Abakumov, *Nature Communications* 3 (2012) 1163–1167.
  - [21] S. Petitgirard, A. Salamat, P. Beck, G. Weck, P. Bouvier, *Journal of Synchrotron Radiation* 21 (1) (2014) 89–96.
  - [22] M. D. Knudson, M. P. Desjarlais, *Physical Review Letters* 103 (22) (2009) 5–8.
  - [23] M. Koenig, E. Henry, G. Huser, A. Benuzzi-Mounaix, B. Faral, E. Martinolli, S. Lepape, T. Vinci, D. Batani, M. Tomasini, B. Telaro, P. Loubeyre, T. Hall, P. Celliers, G. Collins, L. DaSilva, R. Cauble, D. Hicks, D. Bradley, A. MacKinnon, P. Patel, J. Eggert, J. Pasley, O. Willi, D. Neely, M. Notley, C. Danson, M. Borghesi, L. Romagnani, T. Boehly, K. Lee, *Nuclear Fusion* 44 (12) (2004) S208–S214.
  - [24] S. H. Glenzer, R. Redmer, *Reviews of Modern Physics* 81 (4) (2009) 1625–1663.
  - [25] M. G. Gorman, R. Briggs, E. E. McBride, A. Higginbotham, B. Arnold, J. H. Eggert, D. E. Fratanduono, E. Galtier, A. E. Lazicki, H. J. Lee, H. P. Liermann, B. Nagler, A. Rothkirch, R. F. Smith, D. C. Swift, G. Collins, J. S. Wark, M. I. McMahon, *Physical Review Letters* 115 (9) (2015) 095701.
  - [26] L. Fletcher, H. Lee, T. Döppner, E. Galtier, B. Nagler, P. A. Heimann, C. Fortmann, S. LePape, T. Ma, M. Millot, A. Pak, D. Turnbull, D. A. Chapman, D. Gericke, J. Vorberger, T. G. White, G. Gregori, M. Wei, B. Barbreil, R. W. Falcone, C. Kao, H. Nuhn, J. Welch, U. Zastrau, P. Neumayer, J. B. Hastings, S. H. Glenzer, *Nature Photonics* 9 (4) (2015) 274–279.
  - [27] O. T. Lord, I. G. Wood, D. P. Dobson, L. Vočadlo, W. Wang, A. R. Thomson, E. T. H. Wann, G. Morard, M. Mezouar, M. J. Walter, *Earth and Planetary Science Letters* 408 (2015) 226–236.
  - [28] D. Kraus, A. Ravasio, M. Gauthier, D. O. Gericke, J. Vorberger, S. Frydrych, J. Helfrich, L. Fletcher, G. Schumann, B. Nagler, B. Barbreil, B. Bachmann, E. J. Gamboa, S. Göde, E. Granados, G. Gregori, H. Lee, P. Neumayer, W. Schumaker, T. Döppner, R. W. Falcone, S. H. Glenzer, M. Roth, *Nature Communications* 7 (2016) 10970.
  - [29] G. Weck, F. Datchi, G. Garbarino, S. Ninet, J. A. Quey-

- roux, T. Plisson, M. Mezouar, P. Loubeyre, *Physical Review Letters* 119 (23) (2017) 235701.
- [30] M. A. Barrios Garcia, Ph.D. thesis, University of Rochester (2010).
- [31] W. J. Carter, S. P. Marsh, S, Tech. rep., Los Alamos (1977).
- [32] S. P. Marsh, LASL Shock Hugoniot Data, University of California Press (1980).
- [33] B. Meyer, G. Thiell, *Physics of Fluids* 27 (1) (1984) 302.
- [34] D. E. Fratanduono, T. R. Boehly, P. M. Celliers, M. A. Barrios, J. H. Eggert, R. F. Smith, D. G. Hicks, G. Collins, D. D. Meyerhofer, *Journal of Applied Physics* 110 (7) (2011).
- [35] D. A. Chapman, Ph.D. thesis, University of Warwick (2015).
- [36] D. A. Chapman, Tech. rep., AWE Report 12/17, AWE (2017).
- [37] L. Ornstein, F. Zernike, *Proc. Akad. Sci.* 17 (1914) 793.
- [38] K. Wünsch, J. Vorberger, G. Gregori, D. O. Gericke, *Journal of Physics A* 42 (21) (2009) 214053.
- [39] N. D. Mermin, *Physical Review B* 1 (5) (1970) 2362–2633.
- [40] G. Kresse, J. Hafner, *Physical Review B* 47 (1) (1993) 558–561.
- [41] G. Kresse, J. Hafner, *Physical Review B* 49 (20) (1994) 14251–14269.
- [42] G. Kresse, J. Furthmuller, *Computational Materials Science* 6 (15) (1996).
- [43] G. Kresse, J. Furthmuller, *Physical Review B* 54 (16) (1996) 11169.
- [44] D. Kraus, J. Vorberger, D.O. Gericke, V. Bagnoud, A. Blažević, W. Cayzac, A. Frank, G. Gregori, A. Ortner, A. Otten, F. Roth, G. Schaumann, D. Schumacher, K. Siegenthaler, F. Wagner, K. Wünsch, M. Roth, *Physical Review Letters* 111 (25) (2013) 255501.
- [45] K. Wünsch, J. Vorberger, D. O. Gericke, *Physical Review E* 79 (1) (2009) 010201.
- [46] T. Ma, L. B. Fletcher, A. Pak, D. A. Chapman, R. W. Falcone, C. Fortmann, E. Galtier, D. O. Gericke, G. Gregori, J. B. Hastings, O. L. Landen, S. Le Pape, H. Lee, B. Nagler, P. Neumayer, D. Turnbull, J. Vorberger, T. G. White, K. Wünsch, U. Zastra, S. H. Glenzer, T. Döppner, *Physics of Plasmas* 21 (5) (2014) 056302.
- [47] C. Prescher, V. B. Prakapenka, *High Pressure Research* 35 (3) (2015) 223–230.
- [48] L. Fontana, D. Q. Vinh, M. Santoro, S. Scandolo, F. A. Gorelli, R. Bini, M. Hanfland, *Physical Review B* 75 (17) (2007) 174112.
- [49] D. Kraus, J. Vorberger, J. Helfrich, D. O. Gericke, B. L. Bachmann, V. Bagnoud, B. Barbreil, A. Blažević, L. B. Fletcher, A. Frank, S. Frydrych, E. J. Gamboa, M. Gauthier, E. Granados, G. Gregori, N. J. Hartley, B. Kettle, H. J. Lee, B. Nagler, P. Neumayer, M. M. Notley, A. Ortner, A. Otten, A. Ravasio, D. Riley, F. Roth, G. Schaumann, D. Schumacher, W. Schumaker, K. Siegenthaler, C. Spindloe, F. Wagner, S. H. Glenzer, M. Roth, R. W. Falcone, *Physics of Plasmas* 22 (2015) 056307.
- [50] J. Vorberger, J. K. U. Plageman and R. Redmer, (under review).
- [51] C.E. Starrett, D. Saumon, *Physical Review E* 92 (3) (2015) 033101.
- [52] T. Kluge, C. Rödel, M. Rödel, A. Pelka, E. E. McBride, L. B. Fletcher, M. Harmand, A. Krygier, A. Higginbotham, M. Bussmann, E. Galtier, E. Gamboa, A. L. Garcia, M. Garten, S. H. Glenzer, E. Granados, C. Gutt, H. J. Lee, B. Nagler, W. Schumaker, F. Tavella, M. Zacharias, U. Schramm, T. E. Cowan, *Physics of Plasmas* 24 (10) (2017) 102709.
- [53] D. A. Chapman, D. O. Gericke, *Physical Review Letters* 107 (16) (2011) 165004.
- [54] N. D. Mermin, *Physical Review* 137 (5A) (1965) A1441.
- [55] P. E. Blöchl, *Physical Review B* 50 (24) (1994) 17953–17979.
- [56] G. Kresse, D. Joubert, *Physical Review B* 59 (3) (1999) 1758.
- [57] J. P. Perdew, K. Burke, M. Ernzerhof, *Physical Review Letters* 77 (3) (1996) 3865.
- [58] S. Nose, *Progress of Theoretical Physics Supplement* (103) (1991) 46.
- [59] J. Vorberger, D. O. Gericke, *Physical Review E* 91 (3) (2015) 033112.